Performance evaluation of strain field measurement by digital image correlation using HEVC compressed ultra-high speed video sequences

Tarek Eseholi, Delphine Notta-Cuvier, François-Xavier Coudoux, Patrick Corlay, Frédéric Robache, Maxence Bigerelle

PERFORMANCE EVALUATION OF STRAIN FIELD MEASUREMENT BY DIGITAL IMAGE CORRELATION USING HEVC COMPRESSED ULTRA-HIGH SPEED VIDEO SEQUENCES

T. Eseholi[+], D. Notta-Cuvier, F-X. Coudoux [+], P. Corlay[+], F. Robache*, M. Bigerelle**

([+]) IEMN UMR 8520, (*) LAMIH UMR 8503, University of Valenciennes, Le Mont Houy, 59313 VALENCIENNES CEDEX (FRANCE)

ABSTRACT

The tremendous growth of imaging applications for mechanical engineering increases the amount of image and video data used to capture the microstructural characteristics or mechanical behavior of materials as a sequence of frames. In this paper, we evaluate the performance of the new state-of-the-art High Efficiency Video Coding (HEVC) standard to compress efficiently video sequences of materials under tensile testing captured with ultra-high speed camera. Different lossless and lossy coding modes are considered and the compression ratios as well as reconstructed video quality are studied. Preliminary simulation results show that HEVC offers high coding efficiency and excellent reconstructed video quality expressed in terms of PSNR as well as SSIM while preserving data accuracy for the prediction of material tensile behavior at high loading speed. We also propose a discussion on the consequences of HEVC compression on image content analysis. We show that material strain's measurements are not affected by HEVC compression in a significant way.

Index Terms— Mechanical Engineering, Digital Image Correlation, Digital Video Compression, High Efficiency Video Coding (HEVC), Image Analysis.

1. INTRODUCTION

Images and visual information constitutes nowadays one of the most dominant channels for acquiring, processing and communicating information in many sectors including entertainment, medicine, meteorology, transportation systems, or physics [1,2]. In particular, mechanical engineering generates a huge amount of visual media to be processed and stored for further use. These include for instance high spatial resolution tomographic still images or ultra-high-speed video imagery for material crash analysis [3]. However, it is common in mechanical engineering to store raw visual data without applying any compression at all, or lossless compression only. But lossless compression leads to limited compression ratios and lossless compressed data still require too large storage devices (several tens or even hundreds of terabytes). An alternative solution to significantly increase the coding efficiency should be to apply lossy compression algorithms such as JPEG or JPEG2000 for still images, or H.264/AVC or HEVC for video sequences [4-6]. Unfortunately, compression artifacts introduced by these algorithms not only affect the visual quality of an image, but can also distort the features that one computes for subsequent tasks related to image analysis or pattern recognition. Since imaging technologies are widely used to analyze the mechanical properties of materials, the image quality considerations have become essential, because of the central paradigm that materials properties are largely dependent on microstructures which don't accept relevant differences between the original and reconstructed data. Hence, only lossless or nearly lossless compression techniques should be considered.

In this paper we focus on the study of dynamic behavior of a material subjected to axial or shear test at high loading speed. In order to track the evolution of displacement and strain fields over the specimen surface (Region of Interest - ROI) throughout loading, a high-speed video camera (up to 25,000 fps) films the ROI. Then, the obtained image sequences are post-processed by Digital Image Correlation (DIC) software to extract mechanical fields [7]. We propose to compress these sequences using HEVC, which constitutes nowadays the state-of-the-art video compression standard, and evaluate the impact of HEVC compression on the performance of the subsequent mechanical analysis. The paper is organized as follows: first, the aim of our study is presented from a mechanical point of view. The measured physical parameters are described as well as the software tools used for their determination [8]. Section 3 gives an overview of the HEVC (High Efficiency Video Coding) compression standard as well as its main innovative coding tools. Then, simulation results for different ultra-high-speed video contents are presented and discussed in detail. In particular, we evaluate the performances in terms of compression ratio, reconstructed video quality as well as precision of measured mechanical parameters and show that HEVC compression doesn't affect the efficiency of the analysis of mechanical properties, i.e. coding artifacts don't interfere with strain measurements. Finally, Section 5 gives the conclusions and further work.

2. STRAIN MEASUREMENTS IN MECHANICAL ENGINEERING

Aiming at predicting the behavior of structures subjected to severe loading conditions such as crash or impact, a first step is to characterize material mechanical behavior over a wide range of strain rate in order to propose accurate behavior models. At the scale of the specimen, the material mechanical response (in terms of true stress vs strain curve) is obtained by performing several tests, including uniaxial tensile test or Arcan shear test, at different loading speed. In such tests, strain measurement is a key point. Indeed, strain fields can become heterogeneous from the very early stages of loading, especially at high test speed (due to fast necking development, in particular). In that case, "global" strain measurement (i.e. strains computed from the measured elongation of a more or less extended area on the ROI, for instance by strain gauge or optical extensometry) is not sufficient to characterize material behavior with a satisfying accuracy and local strain measurement is needed. Local strain measurement means that true strain components are acquired over zones of interest (ZOI) of small dimensions compared to the whole ROI, so that all strain field heterogeneities (strain localization, gradient…) can be known, thus providing an enriched information on material behavior. In that context, Digital Image Correlation technique (DIC) [3] is a very useful tool for displacement field measurement and in-plane strain field computation. In practice, a random pattern is created on the whole specimen ROI by applying sprays of black paint after the specimen surface is painted in white. Grayscale images of the pattern are recorded throughout the loading at constant time interval (depending on camera frame rate). For DIC analysis, a reference image is chosen at a non-deformed stage, just before load is applied to the specimen. Sequences of images are then analyzed using a DIC software (VIC 2D here). First, the random pattern of the reference image is divided into square facets of a few pixels size, each of them being characterized by a unique signature in gray level. This unique signature allows the tracking of facets by DIC software, using a correlation algorithm between each image, recorded at a given instant of loading, and the reference image. This way, in-plane displacements of all facet centers are determined, with respect to their position in the reference image. In-plane strains are finally computed in all facets by spatial derivation. In the present study, DIC technique is applied to displacement/strain field measurement during dynamic uniaxial tensile loading of a polypropylene (PP), at a displacement rate of 1m/s and at room temperature. Testing device is Instron 65/20 hydraulic jack (i.e. 65 kN load cell sensor, maximum speed 20 m.s-1). For the present tests on polymeric material, a piezoelectric load cell sensor, calibrated in the range 0-5kN, with a precision of 2.5 N, is fixed on the rigid frame of the jack. High-speed camera is Photron FASTCAM-APX RS and the frame rate is fixed at 25,000 im/s. 71 images are recorded during the loading, up to specimen failure (test duration of 2.84 µs, nominal axial strain at break of about 6%). In uniaxial tensile tests, longitudinal and transverse strains are the two main components of the in-plane stress tensor, while shear stress remains very low. In order to test the influence of image compression on other kinds of mechanical response, DIC image sequences recorded during Arcan test at 45° of Sikapower® polymeric glue were also considered (Figure 2). In Arcan 45° test, shear strain actually developed significantly in materials.

Figure 1.First image at undeformed stage of dynamic PP tensile specimen (global size of 512x472 pixels vs. useful part of 128x384 pixels).

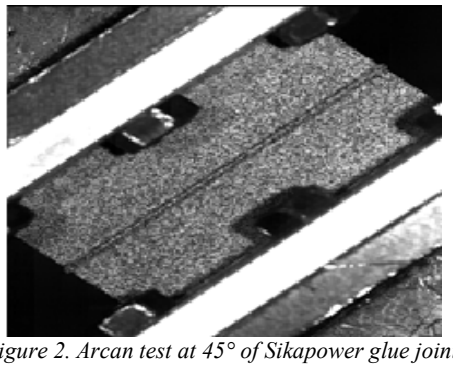

Figure 2. Arcan test at 45° of Sikapower glue joint.

3. BRIEF OVERVIEW OF HEVC

Figure 3 shows the block diagram of the new state-of-the-art H.265/HEVC video coding standard [6]. Like its predecessor known as H.264/AVC, HEVC is based on a hybrid motion-compensated block-based transform video coding scheme including spatial and temporal prediction, transform and quantization of prediction error, as well as entropy coding [9]. However, several improvements have been introduced in the main structure of HEVC, which allow HEVC roughly to double the compression ratio at the same visual quality compared to H.264/AVC [9, 10]. The main innovative features of HEVC are:

- HEVC supports a large variety of block sizes: each frame is divided into Largest Coding Units (LCUs) ranging from 64x64 down to 4x4 samples using flexible recursive square or rectangular sub-partitioning mechanisms.

- The number of intra prediction modes is extended to 35 modes instead of 11 modes in H.264/AVC, hence limiting the intra prediction residual error.
- Other improvements also include the sample adaptive offset (SAO) filter, Adaptive Loop Filtering (ALF) or the Merge mode for motion vector coding [10, 11].

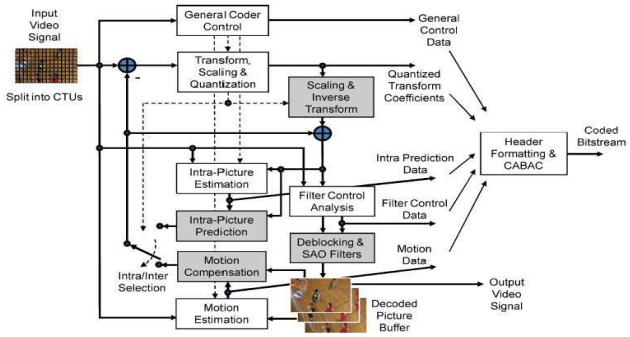

Figure 3. HEVC encoder block diagram (from [9]).

4. SIMULATION RESULTS

In this Section, we aim at studying the impact of HEVC compression of DIC image sequences on the computation of in-plane strain fields during mechanical test. To do that, simulations have been performed on ultra-high speed test video sequence recorded during dynamic tensile test of PP specimen (`Sequence1`, 86 frames of 512x472 pixels each, 25,000fps). It is worth noting that the useful part of the frames, i.e. corresponding to specimen image, is actually of 128x384 pixels while other parts of the frames are composed of black background or white text, added by the software during image recording (Figure 1). Therefore, frames contain mostly homogeneous contents. In order to test HEVC compression on more textured frames, `Sequence2`, registered during Sikapower Arcan test (Figure 2, e.g.) was also considered (150 frames of 512x696 pixels each, 500fps). These sequences are first compressed by means of HEVC, and the Bit-rate as well as the quality of the reconstructed video sequences are both evaluated. The well-known Peak Signal-to-Noise Ratio (PSNR) expressed in dB and Structural Similarity Index Measurement (SSIM) metrics are used for video quality evaluation. The SSIM metric varies between 0 (bad quality) and 1(perfect). It is common in broadcast applications to consider that a PSNR value higher than 35dB corresponds to an excellent video quality. The JVT reference software HM version 10.1 is used for HEVC compression. The Main Profile with Random Access configuration is used [12]. A Clean Random Access (CRA) configuration was selected. The Group of Picture (GOP) size was set to 8 pictures (B-Frames) combined with an Instantaneous Decoding Refresh (IDR) picture (I-Frame), and the coding order was set to 0, 8, 4, 2, 1, 3, 6, 5, and 7, the Reference Frames was = 4. The target quantizer is variable, with a Quantization Parameter QP = 0, 1, 2, 3, 4, 5, 6, 12, 17, 20, 22, 25, 27, 32, and 37. The Intra Period was set to (-1) implies that only the first frame will be coded as Intra. Lossless compression results are also given here as a reference with perfect reconstruction (PSNR= Inf, and SSIM=1). Table I summarizes the HM reference software encoder configuration.

TABLE I – HM 10.1 ENCODING PARAMETERS

CODING OPTIONS	CHOSEN PARAMETER
Encoder Version	HM 10.0
Profile	Main
Reference Frames	4
R/D Optimization	Enabled
Motion Estimation	TZ search
Search Range	64
GOP	8
Hierarchical Encoding	Enabled
Temporal Levels	4
Decoding Refresh Type	1
Intra Period	-1
Deblocking Filter	Enabled
Coding Unit Size/Depth	64/4
Transform Unit Size(Min/Max)	4/32
TransformSkip	Enabled
TransformSkipFast	Enabled
Hadamard ME	Enabled
Asymmetric Motion Partitioning (AMP)	Enabled
Fast Encoding	Enabled
Fast Merge Decision	Enabled
Sample adaptive offset (SAO)	Enabled
Rate Control	Disabled
Internal Bit Depth	8

To turn the encoder into the lossless compression mode, the *Lossless Coding* configuration parameters are enabled causing the transformation, quantization, and all the in-loop filtering operations to be bypassed [14]. Table II summarizes the results obtained for the two sequences noted `Sequence1` and `Sequence2` in terms of bit-rate expressed in bits per pixel (bpp) as well as reconstructed video quality. For lossless coding, the bit-rate for both sequences are 0.66 bpp and 2.3 bpp, respectively. For lossy compression, the video sequences are compressed with a bit-rate varying from 0.005 bpp to 0.66 bpp for `Sequence1`, and from 0.01 bpp to 2.3 bpp for `Sequence2`. These differences are directly related to the spatio-temporal characteristics of video contents.

TABLE II – HEVC COMPRESSION PERFORMANCES

Test Sequences	Y_PSNR (dB)		SSIM		Bit-rate (bpp)	
	Seq1	Seq2	Seq1	Seq2	Seq1	Seq2
Lossless	Inf	Inf	1	1	0.66	2.3
Lossy-QP0	75.6	67.44	1	0.9999	0.66	2.2
Lossy-QP5	60.3	54.42	0.9996	0.9987	0.47	1.43
Lossy-QP12	53.1	47.4	0.9983	0.9962	0.2	0.48
Lossy-QP17	49.2	44.25	0.9965	0.9940	0.09	0.25
Lossy-QP20	47.4	42.6	0.9950	0.9917	0.05	0.133
Lossy-QP22	46	41.3	0.9936	0.9900	0.03	0.1
Lossy-QP25	44.2	39.24	0.9908	0.9853	0.02	0.07
Lossy-QP27	43	37.7	0.9884	0.9819	0.015	0.06
Lossy-QP32	39.9	33.4	0.9770	0.9647	0.007	0.03
Lossy-QP37	37	29.4	0.9562	0.9278	0.005	0.01

The PSNR decreases to minimal values of 37 dB and 29.4 dB for `Sequence1` and `Sequence2`, respectively. The SSIM values reach the minimal values of 0.9562 and 0.9278 for `Sequence1` and `Sequence2`, respectively. The R-D curves for the two video sequences are shown in Figure 4. We can note that the compression efficiency is significantly higher for `Sequence1`, as the corresponding video content is of low complexity and very easy to encode.

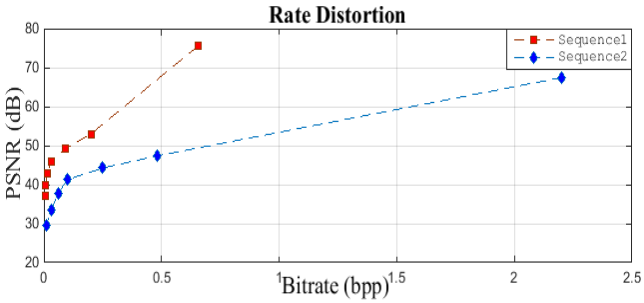

Figure 4. R-D curves for the two video sequences.

Such PSNR and SSIM values correspond to high visual quality levels, as illustrated in Figures 5 and 6 for the QP value QP=25.

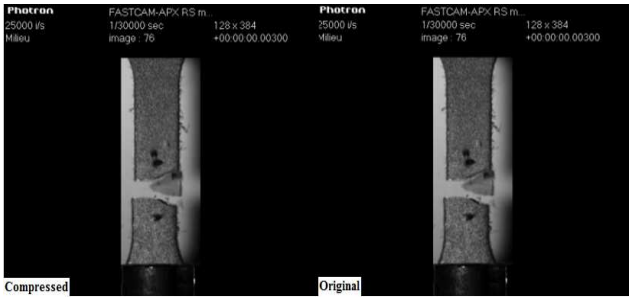

Figure 5. Illustration of HEVC high quality performances for compressed `Sequence1` (QP=25, PSNR =44.4dB and SSIM=0.99, left) compared with the original version (right).

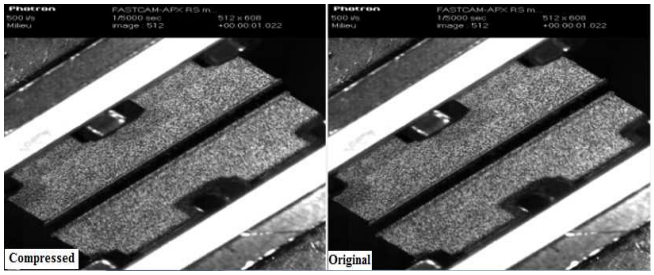

Figure 6. Illustration of HEVC high quality performances for compressed `Sequence2` (QP=25, PSNR =39.2dB and SSIM=0.98, left) compared with the original version (right).

Moreover, the SSIM variations between 1.0 and 0.9853can be considered as irrelevant: hence, HEVC compression preserves very well the structural properties of this kind of image contents which are crucial for further mechanical analysis of material's strain measurements. To illustrate this point, true in-plane strain fields are computed using DIC Software (VIC 2D) based on HEVC compressed images of Sequence 1 (i.e. dynamic tensile test of PP) and Sequence 2 (i.e. Arcan test of glue joint), for lossless sequence and all values of QP. In-plane strains thus computed are compared to those obtained from initial uncompressed image sequence. It is worth noting that strains computed from Lossless image sequence are identical to reference strains computed from initial uncompressed images for both Sequences 1 and 2. Dealing with Sequence 1, Figures 7 to 10 shows examples of relative gaps, $\Delta\varepsilon_{yy}$, between true axial strain computed by DIC technique based on a given Lossy sequence (QP=0, 5, 20 and 25 in those Figures), ε_{yy}^{L}, and true axial strain computed from uncompressed images, ε_{yy}^{ref}, with : $\Delta\varepsilon_{yy} = \dfrac{\varepsilon_{yy}^{L} - \varepsilon_{yy}^{ref}}{\varepsilon_{yy}^{ref}}$

Relative gaps are computed at each stage of loading, i.e. for each recorded image (time step of 0.04 µs) and on 18 selected centers of DIC facets. Those points are all located at the half width of the ROI but with ordinates (i.e. position along specimen axis) varying by step of 10 pixels, point 1 being the upper point on the ROI (i.e. the closest point to the top jaw) and point 18 being the lowest point on the ROI (i.e. the closest point to the bottom jaw, at 170 pixels from point 1, approximately20 mm). First, it appears that relative gaps, $\Delta\varepsilon_{yy}$, can be very important in the first stages of loading. Yet, this trend must be analyzed carefully since in the first stage gaps are computed considering very low strain levels, leading to possibly high value of relative gaps even for acceptable variation of strain value. In addition, it must be highlighted that reference axial strain (ε_{yy}^{ref}) are significantly affected by noise of measurement in the early stage of loading, again because of very low strain value. At higher strain level, relative gaps tend to stabilize at significantly lower value. Results show that relative gaps increase when increasing the value of QP. However, they always remain lower than 10% (in absolute value) at all considered specimen locations, except for QP=25 where higher gaps are computed for a few points. It can be noted that gaps tend to increase when the distance to ROI center (near point 9) increases. It can be partially explained by the fact that strain localization appeared at the center of the specimen, that is to say that reference axial strains were higher in specimen center than in other areas of the ROI. Then, for a same gap in strain value, relative gaps are lower in ROI center. The same trends are noticed for the transverse strains. Considering that relative gaps inferior to 10% (in absolute value) are satisfying in terms of accuracy of computed strain data, HEVC compression algorithm can therefore be used with QP value up to 20, providing a very

interesting bitrate 0.05bpp on this particular image sequence.

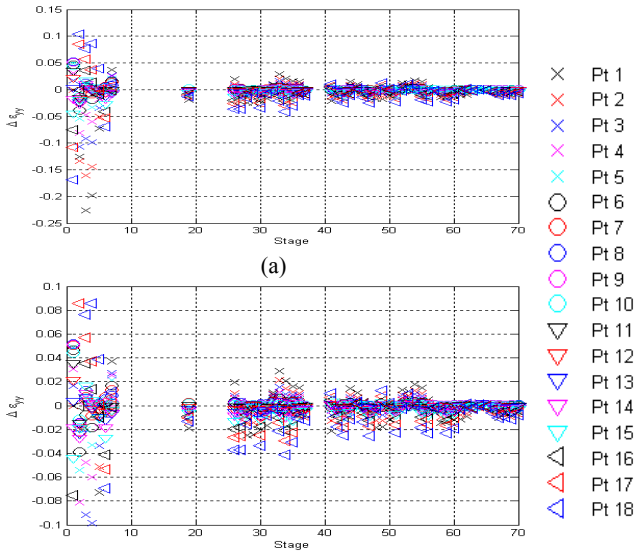

(a)

(b)

Figure 7.Evolution of relative gaps on computed axial strain throughout tensile loading of PP - Case Lossy - QP0. (a) All data (b) Focus on relative gaps between -10% and 10%

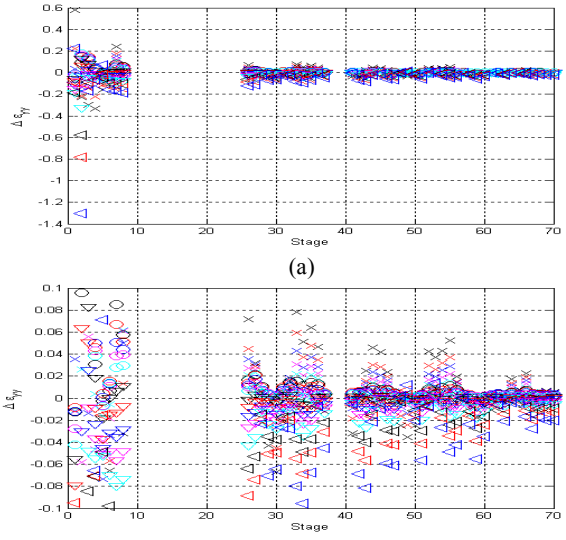

(a)

(b)

Figure 8. Evolution of relative gaps on computed axial strain throughout tensile loading of PP - Case Lossy - QP5. (a) All data (b) Focus on relative gaps between -10% and 10% (For signification of markers see Figure 7)

The same kind of analysis was done for the Sequence 2, i.e. for images recorded during the Arcan shear test of a glue joint. During this test, the three in-plane strain components develop in a significant way. Computation of relative gaps between axial, transverse and shear strain obtained from compressed images at different QP value and Lossless images. As for `Sequence1`, gaps are quite important at the beginning of the loading, due to very low strain levels, and then stabilized at satisfying value (i.e. relative gap lower than 10%), even for the highest values of QP (Figure 11). The comparison of the evolution upon loading of strains computed from sets of images compressed at different QP demonstrates that the compression does not influence the accuracy of results up to QP=20 and only very slightly for QP=25 (Figure 12).

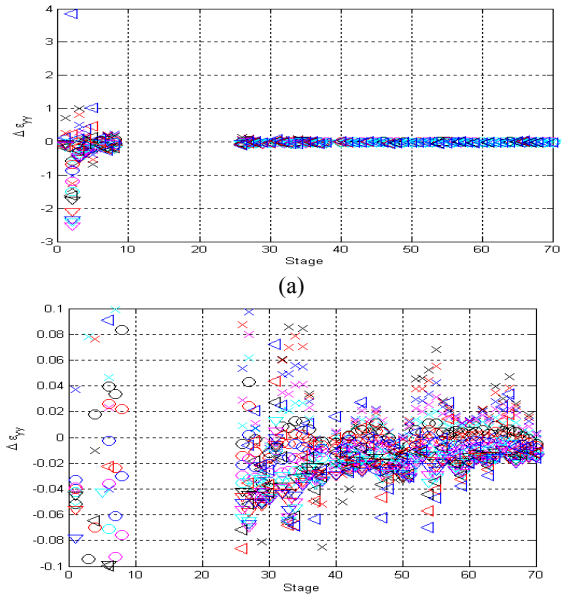

(a)

(b)

Figure 9. Evolution of relative gaps on computed axial strain throughout tensile loading of PP - Case Lossy - QP20. (a) All data (b) Focus on relative gaps between -10% and 10% (For signification of markers see Figure 7).

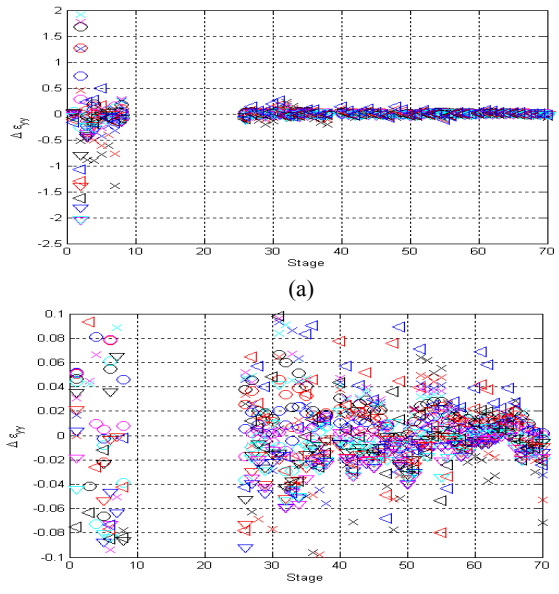

(a)

(b)

Figure 10. Evolution of relative gaps on computed axial strain throughout tensile loading of PP - Case Lossy - QP25. (a) All data (b) Focus on relative gaps between -10% and 10% (For signification of markers see Figure 7).

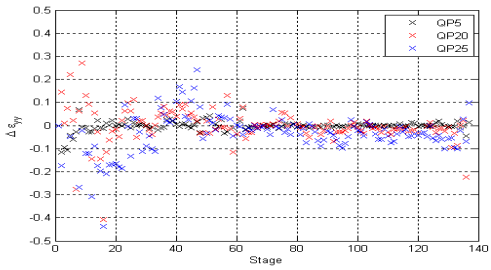

(a)

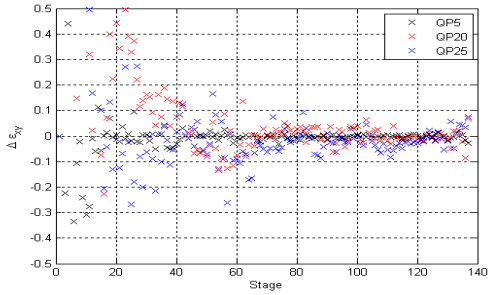

(b)

Figure 11. Evolution of relative gaps between strains computed from Lossy images and Lossless images of Sequence 2 (Arcan shear test of glue joint), in the ZOI of maximal shear strain. (a) Axial strain (b) Shear strain.

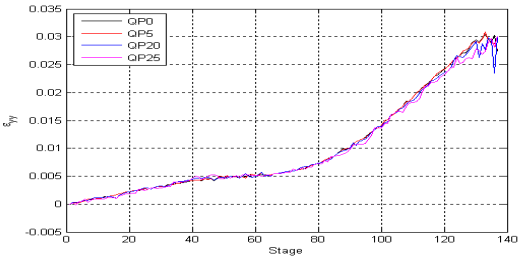

(a)

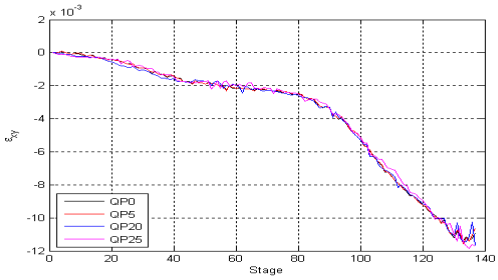

(b)

Figure 12. Evolution upon loading of strains computed from Lossy images and Lossless images of Sequence 2 (Arcan shear test of glue joint), in the ZOI of maximal shear strain. (a) Axial strain (b) Shear strain.

5. CONCLUSION

In this paper, we have evaluated the performance of the state-of-the-art HEVC standard on compression of image sequences of material mechanical response captured by ultra-high speed camera. We have demonstrated that HEVC provides very high coding efficiency as well as high visual quality. Moreover, further image analysis of mechanical response using DIC software showed that material response was very well preserved in the moderately compressed sequences (QP ranging from 0 to 20) with an average SSIM nearly equal to 1 for both frame sequences under test.

6. REFERENCES

[1] R.C. Gonzalez, R.E. Woods, Digital Image Processing, 3rdedition, *Pearson*, 2008.

[2] J.C. Russ, The Image Processing Handbook, 7th edition, *CRC Press*, 2011.

[3] M.A. Sutton, J-J.Orteu, and H.W. Schreier, Image correlation for Shape, Motion and Deformation, Measurements – Basic Concepts, Theory and Applications, *Springer*, 2009.

[4] W. A. Pearlman, A. Said, Digital Signal Compression – Principles and Practice, *Cambridge Press*, 2011.

[5] I.E. Richardson, The H.264 Advanced Video Compression Standard, 2nd edition, *Wiley*, 2010.

[6] V. Sze, M. Bugadavi, G. Sullivan, High Efficiency Video Coding (HEVC) – Algorithms and Architectures, *Springer*, 2014.

[7] A.F. Epee, F. Lauro, B. Bennani, B. Bourel, *Constitutive model for a semi-crystalline polymer under dynamic loading*, Int. J. Solids Struct. 48:1590-1599, 2011.

[8] "VIC-2D Full-Field Deformation Measurement System", Technical datasheet, available on: http://www.correlatedsolutions.com/

[9] G. J. Sullivan, and al., "Overview of the high efficiency video coding (HEVC) standard," *IEEE Trans. Circuits Syst. for Video Technol.*, vol. 22, no. 12, pp. 1649–1668, Dec. 2012.

[10] M. Pourazad, and al., "Hevc: The new gold standard for video compression: How does hevc compare with h.264/avc?," *IEEE Consumer Electronics Magazine*, pp. 36–46, June 2012.

[11] JCTVC-H0083, Method of Frame-based Lossless Coding Mode for HEVC, San Jose, CA, USA, Feb. 2012.

[12] HEVC Reference Software Online: https://hevc.hhi.fraunhofer.de/svn/svn_HEVCSoftware/

[13] J.-R. Ohm. and al., " Comparison of the Coding Efficiency Of Video Coding Standards—Including High Efficiency Video Coding (HEVC)", *IEEE Trans. On Circuits and Systems for Video Technology* 22 (12),1669-1684,December 2012.

[14] ITU-T SG16 WP3 and ISO/IEC JTC1/SC29/WG11. AHG19: A QP-based enabling method for lossless coding in HEVC, JCT-VC document, JCTVC-H0528, San José, CA, Feb. 2012.